Tuning of Sorted Double-Walled Carbon Nanotubes by Electrochemical Charging

Martin Kalbac,*,† Alexander A. Green,‡ Mark C. Hersam,‡ and Ladislav Kavan†

†J. Heyrovský Institute of Physical Chemistry, Academy of Sciences of the Czech Republic, v.v.i., Dolejškova 3, CZ-18223 Prague 8, Czech Republic, and ‡Department of Materials Science and Engineering and Department of Chemistry, Northwestern University, Evanston, Illinois, 60208-3108

ABSTRACT Double-walled carbon nanotubes sorted by density gradient ultracentrifugation were examined by Raman spectroscopy and by *in situ* Raman spectroelectrochemistry. The sorted samples had a narrow distribution of diameters of both inner and outer tubes, which enabled a comparison of the behavior of inner metallic tubes and inner semiconducting nanotubes as a function of the applied electrochemical potential. The metallic inner tubes were efficiently doped even though they were protected from electrolyte ions by the outer wall, whereas the doping of semiconducting inner tubes was observed only at high magnitudes of the electrode potential. These results indicate that the doping response of inner tubes is predominantly controlled by inner tube electronic properties. On the other hand, the effect of electronic structure of the outer tube on the behavior of inner tube is weak. Furthermore, the efficiency of the charge transfer from outer to inner wall depends on the doping level. A low doping level corresponds to a high efficiency of the charge-transfer, while a high doping level shows low charge-transfer efficiency.

KEYWORDS: double-walled carbon nanotubes · electrochemical gating · spectroelectrochemistry

Double-walled carbon nanotubes (DWCNTs) are a special case of multiwalled carbon nanotubes (MWCNTs) since they consist of only one outer tube and one inner tube. DWCNTs exhibit improved performance for several applications (*e.g.,* field effect transistors, polymer composites, field emission, and transparent conductors) compared to single-walled carbon nanotubes (SWCNTs) and MWCNTs, thus motivating a detailed understanding of DWCNT properties. DWCNTs can be prepared by a thermal conversion from fullerene peapods[1] or directly by chemical vapor deposition (CVD). The expeapod DWCNTs are of high quality but this procedure is difficult to scale up. On the other hand, CVD can be used for more efficient DWCNT growth. However, current CVD synthetic protocols fail to produce pure DWCNTs, which are free from SWCNTs and MWCNTs, and thus the studies of the CVD-grown DWCNTs are complicated by the presence of the latter two materials.[2]

Recent progress in density gradient ultracentrifugation (DGU) has enabled efficient sorting of DWCNTs and their separation from SWNTs and MWCNTs.[3] Furthermore, sorted DWCNTs can be obtained with a relatively narrow distribution of diameters.[3] As the diameter of the inner tube is rather strictly defined by the outer diameter, sorting of DWCNTs leads to well-defined samples also from the viewpoint of the inner tubes. In these high purity DWCNT samples, Raman spectroscopy allows a relatively straightforward identification of inner tubes and outer tubes. The frequency of the Raman radial breathing mode (ω_{RBM}) scales with the tube diameter (d_t) according to

$$\omega_{RBM}=A/d_t + B \quad (1)$$

where $A = 217.8$ cm^{-1} · nm and $B = 15.7$ cm^{-1} (ref 4). The RBM thus allows direct evaluation of the diameters of the studied nanotubes from their Raman spectra and thus the low frequency and high frequency RBM bands can be attributed to outer and inner tubes, respectively, in sorted DWCNTs. However, if the sample contains also SWCNTs, it is not as easy to distinguish between inner tubes and small diameter SWCNTs solely from Raman spectroscopy of the as-received samples. Recently, it has been shown that chemical/electrochemical doping together with optical and Raman spectroscopy can be used to solve this problem.[5] It has been shown that doping has a significant effect on the intensity of all Raman modes since charge carriers are introduced into the carbon nanotubes and thus the electronic states are filled or depleted. The simplest model assumes that the filling or depletion of the electronic states, which are involved in the resonance Raman process, leads to strong bleaching of the Raman signal, because optical transitions needed for

*Address correspondence to kalbac@jh-inst.cas.cz.

Received for review July 30, 2009 and accepted December 23, 2009.

Published online January 5, 2010.
10.1021/nn900895w

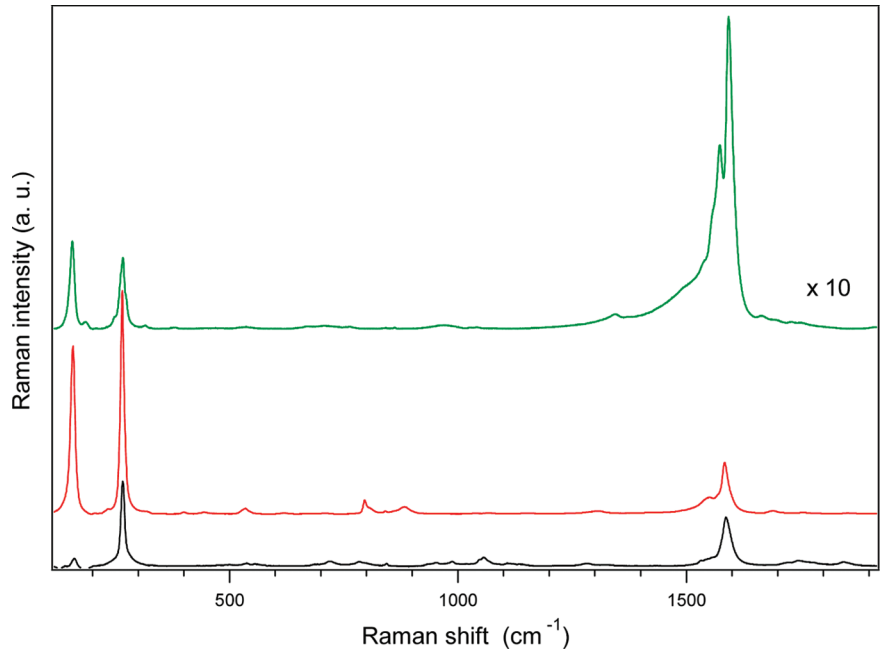

Figure 1. Raman spectra of sorted DWCNTs measured using different laser excitation energies: 2.41 (514 nm), 1.58 (785 nm) and 1.16 eV (1064 nm) (from top to bottom). The spectra are offset for clarity, but the intensity scale is the same for all spectra except for the top spectrum which was zoomed by a factor of 10.

resonance enhancement of Raman spectra are quenched.[6,7] However, recently, it was demonstrated that the filling/depletion of *any* electronic state leads to strong bleaching of the Raman signal.[8,9] The observation of this bleaching effect is independent of whether or not the particular state is involved in the resonance Raman process.[8,9]

In contrast to SWCNTs, the electrochemical doping of DWCNTs is more complex because the inner tube is protected from the environment by the outer tube.[2] Since the inner tube is not in a direct contact with a dopant and/or compensating counterions,[10] any effect of the charge must be mediated electronically between the outer tube and the inner tube. This is usually also the case of chemical doping of a DWCNT where the dopant is located outside the DWCNT.[11,12] This assumption has been confirmed by chemical doping of DWCNTs[10] and also by recent spectroelectrochemical studies of ex-peapod DWCNTs.[5,13,14] However, a detailed evaluation of the specific role of the electronic properties of the inner nanotubes (whether they are metallic or semiconducting) and the efficiency of charge transfer from the outer to the inner wall remains a great challenge.

Here, we present a Raman and an *in situ* Raman spectroelectrochemical study of sorted CVD grown DWCNTs. The narrow distribution of outer and inner diameters of the sorted DWCNTs allows the identification and study of semiconducting and metallic tubes for both inner and outer tubes, which appear in the Raman spectra. By tuning the laser excitation energy, we followed separately the effects of charge on semiconducting and metallic inner tubes, respectively. Furthermore, due to the sample purity, the spectra were not corrupted by MWCNTs and SWCNTs, which allowed unambiguous characterization of effects that are solely attributed to DWCNTs.

RESULTS AND DISCUSSION

Figures 1 and 2 show the Raman spectra excited by three different laser excitation energies for sorted and unsorted DWCNTs, respectively. The RBM region of the unsorted DWCNT sample contains multiple bands, several which likely correspond to SWCNT impurities. For sorted DWCNTs all three spectra are dominated by only two bands at about 265 and 155 cm^{-1}. These two bands correspond to the inner and outer tubes, respectively.[3] It is evident that the analysis of the sorted sample is more transparent as a result of its simpler Raman spectra. Furthermore, the intensities of the RBM bands are about 10 times stronger for the sorted sample than for the unsorted sample, which enables more detailed studies of sorted samples in general. The enhancement of the Raman signal of sorted DWCNT can be rationalized by the improvement of the purity of the sample during the sorting process. We note that the samples are deposited on a substrate, so the rebundling of the tubes is very likely; hence, the enhancement of the Raman signal cannot be attributed solely to isolated tubes.[7]

The Raman spectra excited by different laser excitation energies (Figure 1) exhibit different intensities of the RBM bands. The reason for this effect might be the different electronic transitions which are involved in the resonance effect. (For inner tubes E_{11}^{M}, E_{22}^{S}, and E_{11}^{S} transitions are in resonance with 2.41, 1.57, and 1.16

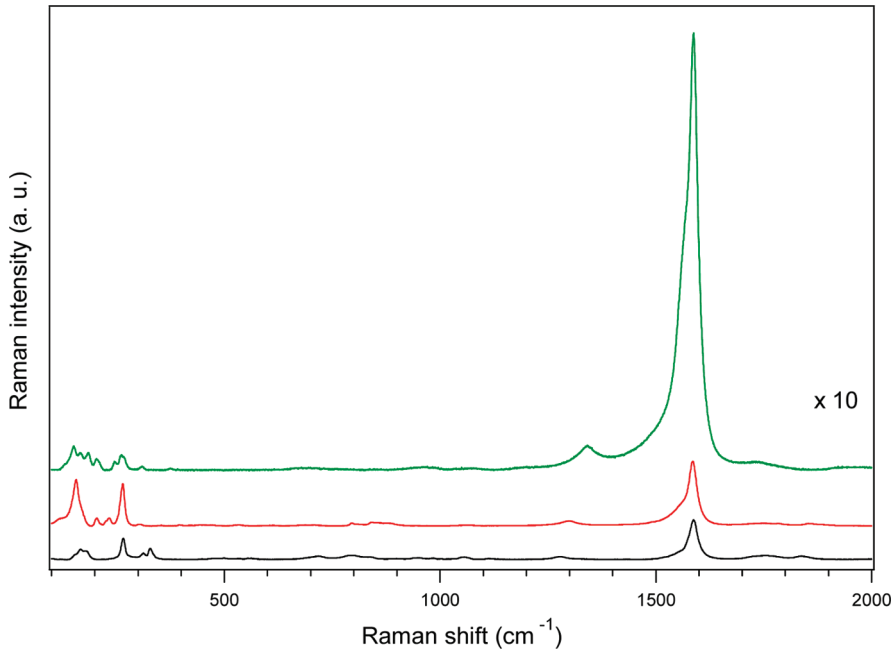

Figure 2. Raman spectra of unsorted DWCNTs measured using different laser excitation energies: 2.41 (514 nm), 1.58 (785 nm) and 1.16 eV (1064 nm) (from top to bottom). The spectra are offset for clarity, but the intensity scale is the same for all spectra except for the top spectrum which was zoomed by a factor of 10.

eV laser energies, respectively. For outer tubes the E_{33}^S, E_{11}^M, and E_{22}^S transitions are in resonance with 2.41, 1.57, and 1.16 eV laser energies, respectively.)

The RBM bands of inner tubes of our sorted DWCNTs do not exhibit a fine structure. The fine structure of the RBM bands of inner tubes was typically observed for expeapod DWCNTs and also for CVD-grown DWCNTs having thin diameter inner tubes.[15] Different positions of the RBM bands are attributed to different pressures that inner tubes experience in different outer tubes.[16] However, for larger diameter inner tubes in DWCNT prepared by CVD growth process, the broader RBM bands of inner tubes were obtained,[17] and fine structure was not observed. This is also the case of the sorted sample studied here. Furthermore, in sorted samples the range of outer tube diameters is limited. This can also reduce the number of the RBM bands associated with one inner tube in different outer tubes.

The tangential displacement (TG) mode of both the sorted and unsorted DWCNT samples is observed in the region of 1450−1630 cm^{-1}. The TG band consists generally of six Raman-active lines: $2A_{1g} + 2E_{1g} + 2E_{2g}$. The number of Raman-active bands is reduced to three for zigzag and armchair tubes. The E_1 and E_2 modes have a much weaker Raman intensity than the totally symmetric A_1 modes.[18] Thus, only two main components of the TG mode are usually observed. This is consistent with our experimental observation for the sorted sample. Two components of the TG mode (the G^+ and the G^- lines) are found at around 1580−1590 and 1550−1570 cm^{-1}, respectively, depending on the laser excitation energy. In the unsorted sample, the two peak-structure is not obvious, probably due to the contribution of tubes with many different diameters.[7] Nevertheless, the diameter dependence of the TG mode frequency is not strong enough to clearly distinguish between contributions from inner tubes and outer tubes even in sorted DWCNT samples. This also complicates the study of the line shape of the TG band of undoped DWCNTs. Later in this study, however, we will show that the contribution of inner and outer tubes to the TG mode can be distinguished in electrochemically charged DWCNT samples, hence the understanding of the line shape of the TG mode can be significantly improved.

Figure 3 shows the optical absorbance of solutions of unsorted DWCNTs specified by the manufacturer

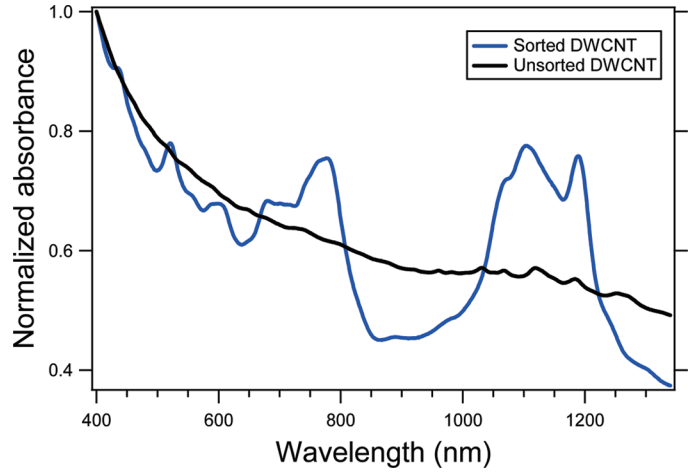

Figure 3. Normalized optical absorbance of solutions of unsorted DWCNTs specified by the manufacturer (Unidym, Inc.) to consist of 60% DWCNTs and sorted DWCNTs produced using density gradient ultracentrifugation (DGU).

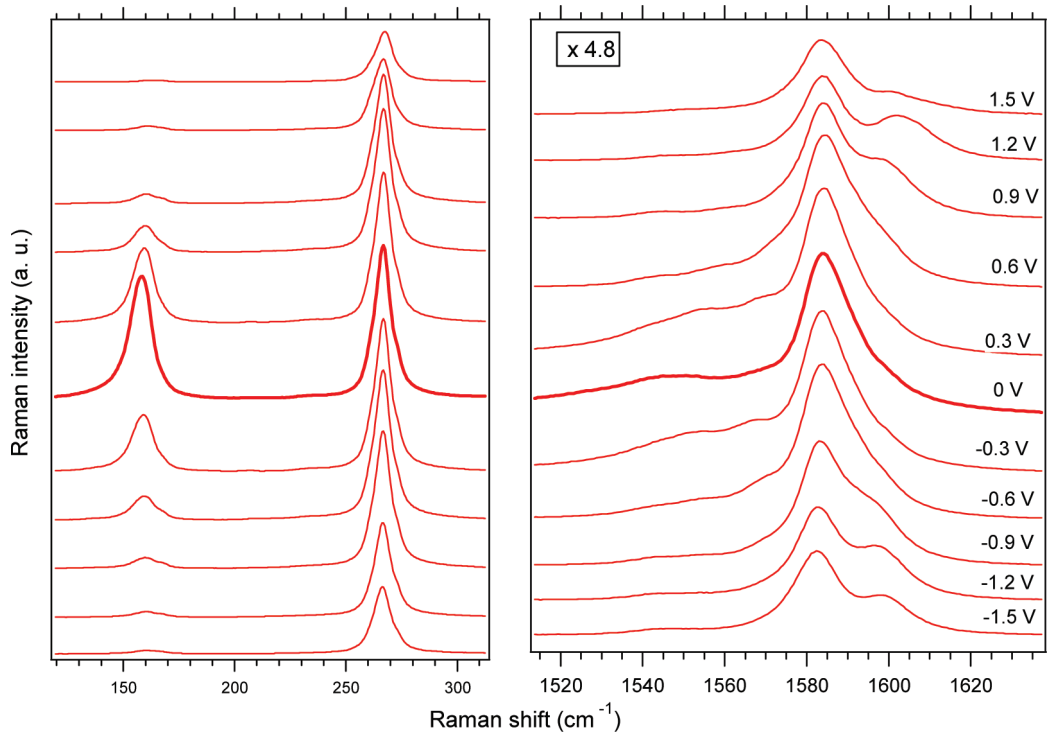

Figure 4. *In-situ* Raman spectroelectrochemical data on sorted DWCNTs in the electrode potential range from −1.5 to 1.5 V *vs* Ag/Ag^+ (bottom to top). The spectra are excited by 1.58 eV (785 nm) laser radiation. The electrochemical potential is labeled on each curve. The spectra are offset for clarity, but the intensity scale is the same for all spectra in the particular window.

(Unidym, Inc.) to consist of 60% DWCNTs and sorted DWCNTs (>98%) produced using density gradient ultracentrifugation (DGU).[3] The optical spectrum of the unsorted DWCNTs contains many weak peaks for wavelengths *ca*. 1000−1300 nm whose assignment is unclear. They are associated with SWCNTs and DWCNTs but the spectrum is dominated by a broad absorbance background, which indicates carbonaceous impurities and possibly very large diameter carbon nanotubes. In contrast, separation of the raw unsorted DWCNT material by density gradient ultracentrifugation causes the emergence of numerous strong absorbance peaks attributable to carbon nanotubes and a significant decrease in the carbonaceous impurity background. These changes in the optical absorbance of the DWCNTs before and after sorting highlight the improvements in sample purity afforded by DGU and the limitations of earlier studies that have relied solely on as-received, CVD-grown DWCNTs.

Figure 4 shows *in situ* Raman spectroelectrochemical data on the sorted DWCNTs. The spectra are obtained from the sample deposited on a substrate, so the rebundling of the tubes is very likely. In our previous studies on SWCNTs,[8,19,20] we observed only weak influence of the bundling on spectroelectrochemical behavior of carbon nanotubes. A typical difference was slight broadening of the Raman intensity/potential profile. This is probably caused by the extension of the resonance window and/or inhomogeneous charge distribution between tubes with different location within a bundle. Nevertheless, these effects are relatively weak and they do not significantly affect the results of our study here.

The spectra on Figure 4 were excited using a 1.58 eV laser excitation energy. According to eq 1, the RBM of the outer tubes (158 cm^{-1}) corresponds to a diameter of about 1.53 nm, while the diameter of inner tubes with the RBM at 265 cm^{-1} is about 0.87 nm. The difference of the diameters is 0.66 nm, which matches the expected double of the graphite-like spacing. Considering the diameters of inner and outer tubes and the Kataura plot,[21] the semiconducting inner tubes and metallic outer tubes are in resonance with the 1.58 eV laser excitation energy.[21] The electrochemical charging leads to the bleaching of the intensity of the Raman signal as can be seen in Figure 4. A more detailed analysis of the RBM region shows that there is an obvious difference in the intensity bleaching of the RBM bands of the inner and outer tubes, respectively. The RBM band assigned to the metallic outer tubes is quickly bleached and at a potential of about ± 1.2 V almost completely vanishes. In contrast, for the Raman intensity of the RBM band assigned to semiconducting inner tubes, the response to the electrode potential is very weak. A large offset in bleaching of about 0.9 V is also found in the latter case. (The intensity of the Raman bands is typically not changed up to a potential of about ± 0.9 V, and then it is strongly bleached.) Furthermore, the RBM band at the maximum applied electrode potential (±1.5 V) still possesses about $^1/_3$ of the intensity of the

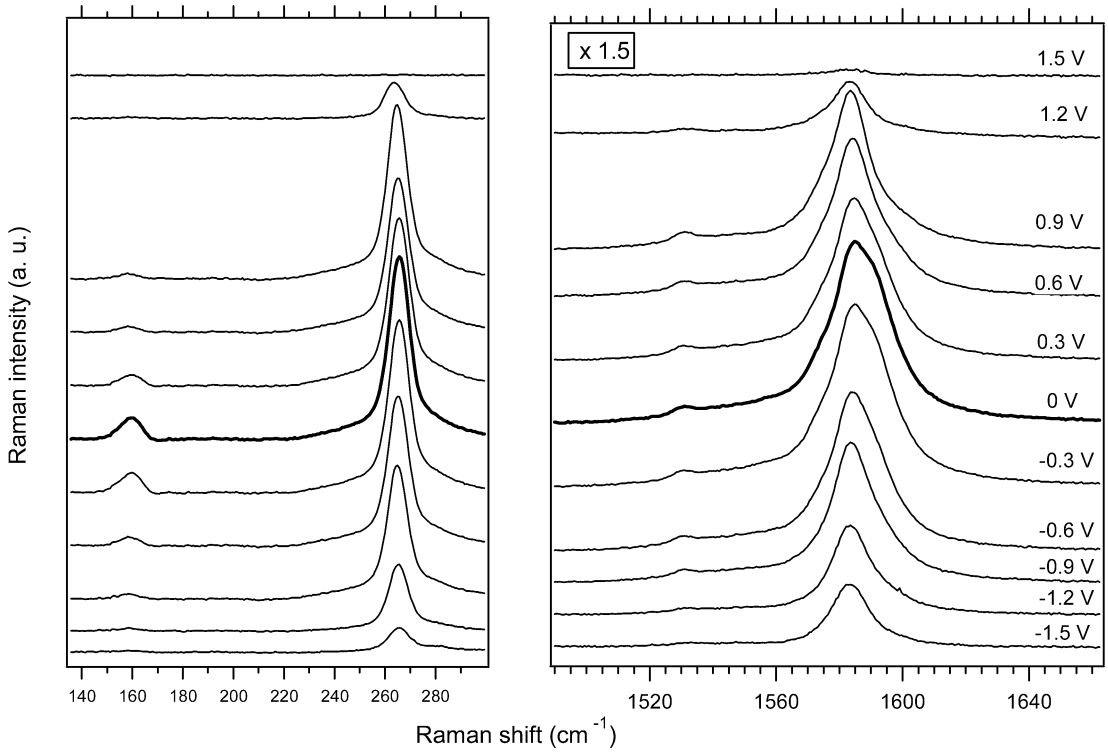

Figure 5. ***In-situ*** **Raman spectroelectrochemical data on sorted DWCNTs in the electrode potential range from −1.5 to 1.5 V *vs* Ag/Ag$^+$ (bottom to top). The spectra are excited by 1.16 eV (1064 nm) laser radiation. The electrochemical potential is labeled on each curve. The spectra are offset for clarity, but the intensity scale is the same for all spectra in the particular window.**

signal at 0 V. The intensity bleaching of the RBM of outer metallic tubes agrees with recent results obtained on SWCNTs.[8] It has been demonstrated that the filling of *any* electronic states of carbon nanotubes causes a significant bleaching of the Raman intensity probably due to broadening of the Raman resonance profile.[8] For metallic tubes, the filling/depletion of the electronic states is expected already when the Fermi level, E_F, is slightly deviated from $E_F = 0$ V. Hence, the bleaching of the Raman modes of metallic tubes is triggered by a very small change in the electrode potential. In contrast, for semiconducting tubes (even in SWCNTs), the bleaching of the signal starts to be significant only if the Fermi level reaches the first Van Hove singularity. Therefore, an offset in the bleaching of the Raman modes is observed.[8]

The semiconducting inner tubes are expected to be in resonance with the 1.58 eV laser excitation energy (Figure 4). Therefore, an offset in the bleaching of the RBM can be expected. Furthermore, the inner tubes can be charged only indirectly through the outer tube. It has been suggested previously that the charge applied on DWCNTs is not evenly distributed between the inner and outer tube.[11] Much more charge is located on the outer tubes. In other words, outer tubes are more strongly affected by the doping than the inner tubes. This effect allows the inner tubes in DWCNTs to be distinguished from narrow SWCNTs having their RBMs at similar frequencies.[5] A combination of the uneven charge distribution between inner and outer tubes together with the semiconducting character of the inner tubes results in a large offset in the doping-driven bleaching of the RBM in the Raman spectra (Figure 4).

The diameter dependence of the TG mode frequency is very weak, so it is difficult to distinguish the TG bands of inner and outer tubes of the DWCNTs in their undoped state. Nevertheless, a different response of inner and outer tubes to doping results in the distinct behavior of inner and outer tubes and therefore the development of the TG mode line shape may be qualitatively understood. We suggest that the metallic outer tubes are represented by a broad TG band centered at about 1550 cm^{-1}. When the magnitude of electrode charge is increased, the band is narrowed and upshifted resulting in a new feature at about 1600 cm^{-1}, which emerges at a potential of ± 0.9 V. On the other hand, we suggest that the predominantly semiconducting inner tubes contribute to the TG band at 1585 cm^{-1}. Indeed, the electrochemical charging does not affect this band significantly due to the large offset in the response of the inner semiconducting tubes to the electrode potential as discussed for the RBM band (*vide infra*). A small contribution of G$^+$ of the outer metallic tubes to the band at 1585 cm^{-1} may cause a slight bleaching of this band at potentials below ±0.9 V.

Figure 5 shows *in situ* Raman spectroelectrochemical data on sorted DWCNTs excited using a 1.16 eV (1064 nm) laser excitation energy. The RBM frequen-

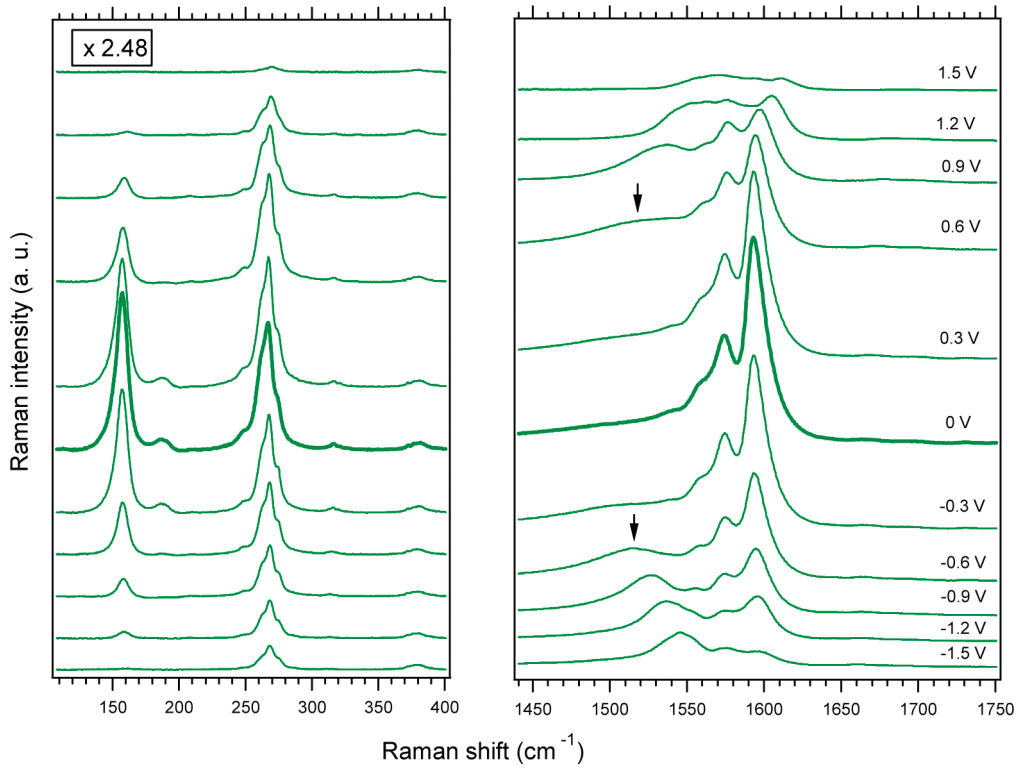

Figure 6. *In-situ* Raman spectroelectrochemical data on sorted DWCNTs in the electrode potential range from −1.5 to 1.5 V *vs* Ag/Ag$^+$ (bottom to top). The spectra are excited by 2.41 eV (514 nm) laser radiation. The black arrows point to the inner tube G$^-$ band, which appears at an electrode potential of ±0.6 V. The electrochemical potential is labeled on each curve. The spectra are offset for clarity, but the intensity scale is the same for all spectra in the particular window.

cies of the outer and inner tubes are 157 and 265 cm^{-1}, respectively. As follows from the Kataura plot,[21] this excitation energy is in resonance with the corresponding optical transitions in semiconducting inner tubes and semiconducting outer tubes. The bleaching behavior of the RBM band of outer tubes mimics the typical behavior of the RBM band of the semiconducting SWCNT.[8] There is an offset in the intensity bleaching (about 0.3 V) and then the RBM attenuates when the magnitude of the electrode potential is increased. The starting intensity of the RBM band is relatively small and thus the signal disappears already at a potential of about ±0.9 V. The RBM signal of the semiconducting inner tubes exhibits a similar offset in the bleaching behavior (about 0.9 V) as in the case of the 1.58 eV laser excitation (Figure 3). A similar bleaching behavior is expected since for both 1.58 and 1.16 eV laser excitation energies the semiconducting inner tubes are in resonance.

The TG mode of DWCNTs in the undoped state (0 V) consists of the main band at about 1585 cm^{-1} and a subtle shoulder at about 1590 cm^{-1} for the 1.16 eV laser excitation energy. The TG mode is suggested to be dominated by the signal of inner tubes; hence, the main feature at 1585 cm^{-1} is assigned to semiconducting inner tubes while the shoulder at 1590 cm^{-1} is assigned to semiconducting outer tubes. The frequency of the TG mode of semiconducting inner tubes is consistent with the assignment of this band to narrow semiconducting tubes. Furthermore, as the magnitude of the electrode potential is increased, the shoulder at 1590 cm^{-1} vanishes. On the other hand, the main feature at 1585 cm^{-1} remains almost intact for potentials below ±1.2 V, which confirms the suggested assignment to the inner semiconducting tubes.

Figure 6 shows *in situ* Raman spectroelectrochemical data on sorted DWCNTs obtained using the 2.41 eV laser excitation energy. The frequencies of the RBM bands of inner and outer tubes are about 266 and 156 cm^{-1}, respectively. Hence, according to the Kataura plot,[21] semiconducting outer tubes and metallic inner tubes are in the resonance for the Raman spectra in Figure 6.

The Raman intensities of the RBM bands of both outer and inner tubes are bleached with increasing magnitude of the electrode potential as expected. Compared to Figure 4, where semiconducting inner tubes are shown, the intensity bleaching behavior of the RBM bands of the inner and outer tubes is much more similar. As mentioned above, for semiconducting tubes, a significant change of the I_{RBM} is found only after the electrode potential exceeds the magnitude of ±0.3 V. For metallic inner tubes, a small deviation of the Fermi level from $E_F = 0$ causes a bleaching of the Raman signal and thus their intensity is bleached relatively rapidly, despite the fact that these inner tubes are shielded by the outer tubes. Obviously, the offset in the bleaching of the RBM band intensity, which is observed for semiconducting tubes but not for metallic tubes, plays an

important role even for inner tubes in DWCNTs. Hence, the RBM band intensity of the metallic inner tubes exhibits faster bleaching as compared to that for semiconducting inner tubes (*cf.* Figure 4 and Figure 6). This observation is consistent with earlier studies of chemical doping of DWCNTs.[12,22]

For the 2.41 eV laser excitation energy, the TG mode part of the spectra is of particular interest since metallic inner tubes are in resonance with this particular laser excitation energy. Even in this study, it is difficult to distinguish the G^- of the inner tubes in the neutral state. However, when the electrode potential is moved from 0 to $\pm$0.6 V, the signal from metallic inner tubes can be distinguished. The G^- band of inner metallic tubes narrows and shifts to higher frequencies as the magnitude of the electrode potential increases to $\pm$1.5 V. This behavior is typical for metallic tubes and recently it has been explained by the Kohn anomaly effect.[23] The Kohn anomaly can be probed by chemical or electrochemical doping. The electrochemical doping fills the states close to the Dirac point and thus the Kohn anomaly effect vanishes, which causes narrowing and upshifting of the G^- band of metallic tubes.[24,25]

To our knowledge, this is the first time that the broadened G^- band has been clearly observed for inner metallic tubes. This experimental result is important since it validates the Kohn anomaly effect in inner metallic tubes. Note that the Kohn anomaly effect appears to be strong for inner metallic tubes. The G^- band can be traced already at potentials of $\pm$0.3 V. At these potentials, the G^- is centered at about 1500 cm^{-1}. Theoretical calculations predict a downshift of the LO mode of metallic tubes to 1500 cm^{-1} for tubes with a diameter of about 0.8 nm.[26] According to eq 1, the diameter of the inner metallic tubes is about 0.87 nm, thus our experimental results are consistent with the latter theoretical predictions.

It is also important to note that the signal of the inner metallic tubes is changed before the Fermi level reaches the Van Hove singularity employed in the Raman resonance effect. The laser excitation energy is in resonance with the E_{11}^M transition of inner metallic tubes which is about 2.4 eV. Therefore, shifts of the Fermi level smaller than $\pm$1.2 eV do not lead to the filling/depleting of the Van Hove singularities which are in resonance with the laser excitation energy (2.41 eV). In other words, the potential window where no change of the intensity is observed should be at least 2.4 V. Note that the change of potential by 1 V leads to a change of the Fermi level by less than 1 eV. (The typical shift of the Fermi level under our experimental conditions is between 0.5$-$0.75 eV.[27]) If we include the latter effect and also unequal charge distribution between the inner and outer tubes, this potential window would be even broader. Furthermore, in the case of inner tubes, the effects of charge are suggested to be mediated solely by the outer tube.[10] Hence, our result confirms that the bleaching of the Raman signal is related to charge injection to electronic states of the carbon nanotube and not to other extrinsic effects such as redistribution of the electrolyte ions surrounding the nanotube.

The behavior of the G^- band during electrochemical charging also seems to be uniform; that is, there is no splitting of the G^- bands. This behavior is important since it indicates that the effect of the electronic structure of the outer tube on the bleaching behavior of the inner tube is weak. A model nanotube sample having all possible chiralities consists of $^2/_3$ semiconducting tubes and $^1/_3$ metallic tubes. A similar distribution may be expected for the outer tubes of DWCNTs. The inner metallic tubes, which are in resonance with the 2.41 eV laser excitation energy, may be accommodated inside the DWCNT with either a semiconducting or metallic outer shell. Hence, assuming a strong influence of the metallic/semiconducting character of the outer tube on the charging behavior of inner tubes, we would expect a different behavior for DWCNTs having metallic outer or semiconducting outer tubes, respectively. This would manifest itself, for example, as a different magnitude of the upshift of the G^- mode for semiconducting and metallic tubes since the shift of this band is very sensitive to the charging. However, the shift of the band is uniform. Therefore, we conclude that the role of the electronic structure of the outer tube on inner tube charging is probably relatively weak.

It is clear that the inner tubes are less affected by electrochemical charging than the outer tubes. This effect is again evident in Figure 7. The plot summarizes the behavior of I_{RBM} for the inner and outer tubes shown in Figures 4 and 6. In addition, the bleaching behavior of SWCNTs (HiPco) with the RBM at about 265 cm^{-1} is shown for comparison. All curves in Figure 7 are normalized to the I_{RBM} at 0 V for the particular tube and laser excitation energy. In every case, the signal of the outer tubes (both metallic and semiconducting) is bleached faster than that for the inner tubes. This also confirms the assignment of the RBM bands to inner and outer tubes. Furthermore, the dramatic difference in the behavior of inner semiconducting and metallic tubes is clearly demonstrated in Figure 7.

For many applications, it is crucial to know how the charge applied on the nanotube wall is transferred to the encapsulated species. Nevertheless, quantitative studies of the charge transfer from the outer tube to the inner tube remain a challenge. As has been shown previously, the bleaching behavior of the Raman signal of SWCNTs depends on $E_{ii} - E_{laser}$, where E_{ii} is the electronic transition which is employed in the resonance effect.[9] Thus, for a given laser excitation energy (E_{laser}), a different bleaching behavior of SWCNTs, which appear in the spectra (having a different chirality and diameter), is expected, since each SWCNT has a slightly different value of $E_{ii} - E_{laser}$. Furthermore, a diameter dependence of the bleaching behavior of the Raman signal has been also reported.[28] Hence, a direct comparison of

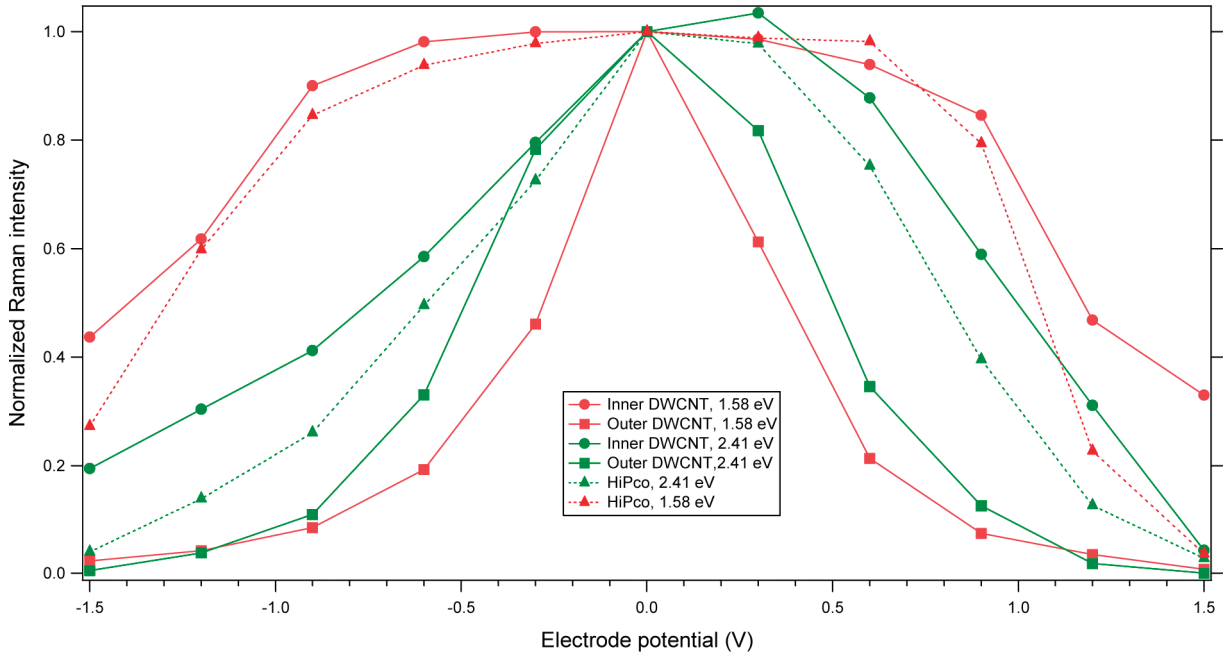

Figure 7. Normalized intensity, I_{RBM} of inner and outer tubes in DWCNTs and HiPco SWCNTs as a function of the electrode potential. The I_{RBM} is referred to the I_{RBM} at 0 V for each particular tube and laser excitation energy. The red and green curves correspond to the spectra excited by 1.58 (785 nm) and 2.41 eV (514 nm) laser energies, respectively. The squares, circles, and triangles correspond to the outer tubes (the RBM at about 155 cm^{-1}), inner tubes (the RBM at about 265 cm^{-1}), and thin SWCNT (the RBM at about 265 cm^{-1}, dashed line), respectively. The lines connect experimental points and serve as a guide for the eye.

the bleaching of the Raman signal of inner and outer tubes may be misleading.

To evaluate the effect of the charge on the behavior of inner tubes, it is desirable to compare the bleaching of inner tubes with similar SWCNTs. The HiPco sample is known to contain a broad diameter distribution of SWCNTs. It also contains SWCNTs with similar RBM band position as the Raman band of the inner tubes in the studied DWCNT sample. According to eq 1, the same positions of the RBM bands in the spectra of SWCNTs and DWCNTs correspond to similar diameters of these tubes assuming that there is no significant effect of the outer tube on the frequency of the RBM band of inner tube. We note that in case of expeapod DWCNTs samples, it is difficult to evaluate the diameter of inner tubes, because there are more bands than expected for the given chiralities within the array of available diameters.[16]

For convenience we also plot the ratio of the intensities of the RBM bands of inner tubes in DWCNT and corresponding SWCNT as a function of the charge per one carbon atom (n). (Figure 8, data are taken from Figure 7.) The transferred charge on the outer tube was calculated from electrode potential (E) assuming an ideal double layer capacitor model according to the equation: $n = CM_CE/F$, where F is Faraday constant, M_C is atomic weight of carbon, and $C = 40$ F/g is specific capacitance.[29]

The circles in Figure 8 represent the ratio of normalized intensities of the RBM band (assigning 1 to be the intensity in pristine form) for metallic inner tubes of DWCNT and a small diameter SWCNT from the HiPco sample (the RBM at about 265 cm^{-1}). The spectra of both samples were excited by the 2.41 eV laser excitation energy. The triangles correspond to the intensity ratio for semiconducting inner tubes of DWCNT and small diameter SWCNTs from the HiPco sample (the RBM at about 265 cm^{-1}). Here, the Raman spectra were excited by the 1.58 eV laser excitation energy.

For metallic tubes, the ratio is increasing, which indicates that the efficiency of the charge transfer is dependent on the actual electrode potential. At an electrode potential of 0.3 V (0.0015e per carbon atom), the ratio of the intensity of the RBM of the inner tube *versus* the intensity of the RBM of the small diameter SWCNT is about 1.1. Hence, the efficiency of the charge transfer from the outer tube to inner tube is more than 90%. On the other hand, at a potential of 1.2 V (0.006e per carbon atom), the ratio of the intensity of the RBM of the inner tube *versus* the intensity of the RBM of the small diameter SWCNT is about 2.5. Therefore, the efficiency of the charge transfer from the outer tube to the inner tube is less than 50%. In contrast, for semiconducting tubes, the ratio is close to 1 up to relatively large electrode potentials (0.9 V (0.0045e per carbon atom) or −1.2 V (0.006e per carbon atom)). This behavior is related to the offset in the bleaching of the Raman intensity of semiconducting tubes. Both narrow semiconducting SWCNTs and semiconducting inner tubes do not change the intensity of Raman modes at low electrode potentials. However, when the electronic states are filled, the change of the intensity is immedi-

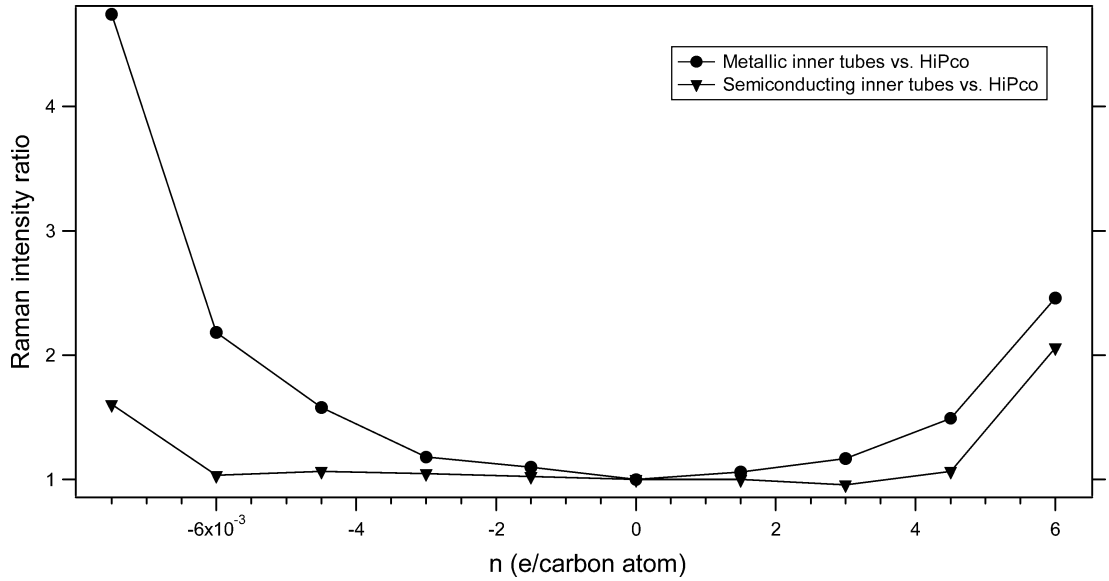

Figure 8. The ratio of normalized Raman intensities of the RBM of semiconducting inner tubes in DWCNTs *vs* the corresponding intensities of SWCNT (HiPco) tubes with the same diameter as a function of the charge per one carbon atom (triangles). The ratio of normalized Raman intensities of metallic inner tubes *vs* the corresponding intensities of HiPco tubes with the same diameter as a function of the charge per one carbon atom (circles). The spectra of the semiconducting and metallic tubes were excited by 1.58 (785 nm) and 2.41 eV (514 nm) laser excitation energies, respectively.

ately observed. At potentials of −1.5 V (−0.0075*e* per carbon atom) and 1.2 V (0.006*e* per carbon atom), the doping efficiency of the inner tubes with respect to the SWCNTs is about 50%.

We note that the previous results obtained from chemical doping suggested an efficiency of the charge transfer to be about 10%.[11] However, in this case, $E_{ii} - E_{laser}$ and the effect of nanotube diameter were not considered. Chemical doping can also lead to high doping levels where the efficiency of charge transfer from outer to inner wall is low.

As can be seen from Figures 4, 5 and 6, the behavior of the TG mode is qualitatively consistent with the behavior of the RBM band. Unfortunately, a detailed quantitative analysis of this band is very difficult. As discussed above, the TG mode consists generally of six Raman-active lines: $2A_{1g} + 2E_{1g} + 2E_{2g}$, which are reduced to only two main components of the TG mode (the G^+ and the G^- lines) in typical Raman spectra. For samples containing different tubes, these two bands (the G^+ and the G^-) in the Raman spectra consist of contributions from many Raman features each coming from a particular (*n*,*m*) tube. The behavior of the TG band at different potentials seems to be chirality- and diameter-dependent which strongly complicates any trials to fit consistently the TG mode for different potentials. From a technical point of view, this band changes its shape, position, and intensity, therefore none of these parameters can be fixed. This results in a large number of possible fits, which do not have physical meaning. For DWCNTs, the situation is even more complex because there are inner and outer tubes which each have a different dependence on electrode potential as we showed for the RBM band. More theoretical studies are obviously needed to provide a solid basis for evaluating the TG mode data for DWCNTs.

CONCLUSION

In conclusion, the effects of the doping on semiconducting and metallic tubes within sorted CVD-grown DWCNTs are examined by *in situ* Raman spectroelectrochemistry. Striking differences in the behavior of inner semiconducting and inner metallic tubes in DWCNTs have been demonstrated. The role of the tube electronic type (*i.e.* semiconducting *versus* metallic) was found to be even stronger than the effect of the outer wall on the inner tube in DWCNTs.

It is shown that metallic inner tubes can be efficiently doped even though they are protected from the electrolyte ions by the outer wall. The efficiency of the charge transfer from outer to inner tube is however dependent on the electrode potential, and it changes from 90% to less than 50% for potentials from 0.3 to 1.2 V or from −0.3 to −1.2 V. Furthermore, in electrochemically doped DWCNTs we were able to observe the G^- band of the inner metallic tubes. This band is of particular importance in studies of doping behavior because it is strongly affected by a Kohn anomaly, which is also confirmed by our study.

The behavior of inner semiconducting tubes is also driven by their electronic structure. In contrast to metallic inner tubes, in the case of the inner semiconducting tubes a strong offset in the bleaching of Raman bands was found. However, when the Fermi level was shifted above the energy of the first Van Hove singularity, the electronic states were filled and the change of the intensity of the RBM band of inner semiconducting tubes was immediately observed. At the potential of −1.5

and +1.2 V, the doping efficiency of the inner tubes with respect to the SWCNTs was about 50%.

Our study also confirms that the dependence of the RBM on electrode potential may be, indeed, used to distinguish between inner tubes of DWCNTs and narrow SWCNTs in the particular sample. However, the differences between the behavior of electronic type of the inner tubes (metallic or semiconducting) and the doping efficiency at different doping levels must be considered.

EXPERIMENTAL DETAILS

The raw material (DWCNT) was purchased from Unidym, Inc., and according to the manufacturer's specification it consisted of 60% DWCNT. The preparation of sorted DWCNTs followed the density gradient ultracentrifugation protocol published previously.[3] The electrodes for *in situ* spectroelectrochemical studies were fabricated by the evaporation of a sonicated ethanolic slurry of sorted DWCNTs on Pt electrodes. The film was outgassed at 80 °C in vacuum and then the electrode was mounted in the Raman spectroelectrochemical cell. The single-compartment spectroelectrochemical cell was airtight and was equipped with a glass optical window for spectroscopic measurements. The HiPco sample was identical to that reported in our previous studies.[29]

The electrochemical cell was assembled in a glovebox (M. Braun); the glovebox atmosphere was Ar containing <1 ppm of both O_2 and H_2O. Electrochemical experiments were carried out using an Autolab PGSTAT (Ecochemie) potentiostat with Pt auxiliary and Ag-wire pseudoreference electrodes; the electrolyte solution was 0.2 M $LiClO_4$ + acetonitrile (both from Aldrich; the latter dried by 4 Å molecular sieve). The Raman spectra were excited by a 2.41 eV mixed Ar^+/Kr^+ laser (Innova 70C series, Coherent), 1.58 eV laser (Sacher Lasertechnik), and a 1.16 eV laser (mpc 6000, Laser Quantum). Spectra were recorded by a Labram HR spectrometer (Horiba Jobin Yvon) interfaced to an Olympus microscope (objective 50×). The laser power impinging on the cell window or on the dry sample was between 1 and 3 mW. The spectrometer was calibrated by the F_{1g} mode of Si at 520.2 cm^{-1}, and the resolution of the spectrometer was about 1 cm^{-1}. The intensity of the Raman spectra was normalized to the excitation laser energy at the sample. Optical absorbance measurements were taken on the DWCNTs in solution using a Cary 500 spectrophotometer (Varian, Inc.). The absorbance of a reference solution containing matching levels of sodium cholate, iodixanol, and water was subtracted from the sample absorbance spectra to ensure that only the optical properties of the DWCNTs were measured.

Acknowledgment. This work was supported by the Academy of Sciences of the Czech Republic (IAA400400911, IAA 400400804, and KAN200100801), Czech Grant agency (203/07/J067), by the Czech Ministry of Education, Youth and Sports (LC-510), by the U.S. National Science Foundation (DMR-0520513, EEC-0647560, and DMR-0706067), and by a Natural Sciences and Engineering Research Council of Canada Postgraduate Scholarship (A.A.G.).

REFERENCES AND NOTES

1. Smith, B. W.; Luzzi, D. E. Formation Mechanism of Fullerene Peapods and Coaxial Tubes: A Path to Large Scale Synthesis. *Chem. Phys. Lett.* **2000**, *321*, 169–174.
2. Iakoubovskii, K.; Minami, N.; Ueno, T.; Kazaoui, S.; Kataura, H. Optical Characterization of Double-Wall Carbon Nanotubes: Evidence for Inner Tube Shielding. *J. Phys. Chem. C* **2008**, *112*, 11194–11198.
3. Green, A. A.; Hersam, M. C. Processing and Properties of Highly Enriched Double-Wall Carbon Nanotubes. *Nat. Nanotechnol.* **2009**, *4*, 64–70.
4. Araujo, P. T.; Doorn, S. K.; Kilina, S.; Tretiak, S.; Einarsson, E.; Maruyama, S.; Chacham, H.; Pimenta, M. A.; Jorio, A. Third and Fourth Optical Transitions in Semiconducting Carbon Nanotubes. *Phys. Rev. Lett.* **2007**, *98*, 067401-1−067401-4.
5. Kalbac, M.; Kavan, L.; Dunsch, L. *In Situ* Raman Spectroelectrochemistry as a Tool for the Differentiation of Inner Tubes of DWCNT and Thin SWCNT. *Anal. Chem.* **2007**, *79*, 9074–9081.
6. Kavan, L.; Dunsch, L. Spectroelectrochemistry of Carbon Nanostructures. *Chemphyschem* **2007**, *8*, 975–998.
7. Kavan, L.; Frank, O.; Green, A. A.; Hersam, M. C.; Koltai, J.; Zolyomi, V.; Kurti, J.; Dunsch, L. *In Situ* Raman Spectroelectrochemistry of Single-Walled Carbon Nanotubes: Investigation of Materials Enriched With (6,5) Tubes. *J. Phys. Chem. C* **2008**, *112*, 14179–14187.
8. Kalbac, M.; Kavan, L.; Dunsch, L. Changes in the Electronic States of Single-Walled Carbon Nanotubes as Followed by a Raman Spectroelectrochemical Analysis of the Radial Breathing Mode. *J. Phys. Chem. C* **2008**, *112*, 16759–16763.
9. Kalbac, M; Farhat, H.; Kavan, L.; Kong, J.; Sasaki, K.; Saito, R.; Dresselhaus, M. S. Electrochemical Charging of Individual Single-Walled Carbon Nanotubes. *ACS Nano* **2009**, *3*, 2320–2328.
10. Cambedouzou, J.; Sauvajol, J. L.; Rahmani, A.; Flahaut, E.; Peigney, A.; Laurent, C. Raman Spectroscopy of Iodine-Doped Double-Walled Carbon Nanotubes. *Phys. Rev. B* **2004**, *69*, 235422-1–235422-6.
11. Chen, G. G.; Bandow, S.; Margine, E. R.; Nisoli, C.; Kolmogorov, A. N.; Crespi, V. H.; Gupta, R.; Sumanasekera, G. U.; Iijima, S.; Eklund, P. C. Chemically Doped Double-Walled Carbon Nanotubes: Cylindrical Molecular Capacitors. *Phys. Rev. Lett.* **2003**, *90*, 257403-1–257403-4.
12. Rauf, H.; Pichler, T.; Pfeiffer, R.; Simon, F.; Kuzmany, H.; Popov, V. N. Detailed Analysis of the Raman Response of N-Doped Double-Wall Carbon Nanotubes. *Phys. Rev. B* **2006**, *74*, 235419-1–235419-10.
13. Kalbac, M.; Kavan, L.; Zukalova, M.; Dunsch, L. *In-Situ* Vis-NIR and Raman Spectroelectrochemistry of Double Wall Carbon Nanotubes. *Adv. Funct. Mat.* **2005**, *15*, 418–426.
14. Kalbac, M.; Kavan, L.; Zukalova, M.; Dunsch, L. Electrochemical Tuning of High Energy Phonon Branches of Double Wall Carbon Nanotubes. *Carbon* **2004**, *42*, 2915–2920.
15. Simon, F.; Kukovecz, A.; Konya, Z.; Pfeiffer, R.; Kuzmany, H. Highly Perfect Inner Tubes in CVD Grown Double-Wall Carbon Nanotubes. *Chem. Phys. Lett.* **2005**, *413*, 506–511.
16. Pfeiffer, R.; Simon, F.; Kuzmany, H.; Popov, V. N. Fine Structure of the Radial Breathing Mode in Double-Wall Carbon Nanotubes. *Phys. Rev. B* **2005**, *72*, 161404-1–161404-4.
17. Ren, W. C.; Li, F.; Chen, J. A.; Bai, S.; Cheng, H. M. Morphology, Diameter Distribution and Raman Scattering Measurements of Double-Walled Carbon Nanotubes Synthesized by Catalytic Decomposition of Methane. *Chem. Phys. Lett.* **2002**, *359*, 196–202.
18. Brown, S. D. M.; Jorio, A.; Corio, P.; Dresselhaus, M. S.; Dresselhaus, G.; Saito, R.; Kneipp, K. Origin of the Breit−Wigner−Fano Lineshape of the Tangential G-Band Feature of Metallic Carbon Nanotubes. *Phys. Rev. B* **2001**, *6315*, 155414-1–155414-8.
19. Kalbac, M.; Kavan, L.; Dunsch, L. *In Situ* Raman Spectroelectrochemistry of SWCNT Bundles: Development of the Tangential Mode During Electrochemical Charging in Different Electrolyte Solutions. *Diamond Relat. Mater.* **2009**, *18*, 972–974.
20. Kalbac, M.; Kavan, L.; Dunsch, L. Effect of Bundling on the Tangential Displacement Mode in the Raman Spectra of

Semiconducting Single-Walled Carbon Nanotubes During Electrochemical Charging. *J. Phys. Chem. C* **2009**, *113*, 1340–1345.
21. Jorio, A.; Araujo, P. T.; Doorn, S. K.; Maruyama, S.; Chacham, H.; Pimenta, M. A. The Kataura Plot Over Broad Energy and Diameter Ranges. *Phys. Status Solidi B* **2006**, *243*, 3117–3121.
22. Barros, E. B.; Son, H.; Samsonidze, G. G.; Souza, A. G.; Saito, R.; Kim, Y. A.; Muramatsu, H.; Hayashi, T.; Endo, M.; Kong, J.; Dresselhaus, M. S. Raman Spectroscopy of Double-Walled Carbon Nanotubes Treated With H_2SO_4. *Phys. Rev. B* **2007**, *76*, 045425-1−045425-11.
23. Lazzeri, M.; Piscanec, S.; Mauri, F.; Ferrari, A. C.; Robertson, J. Phonon Linewidths and Electron-Phonon Coupling in Graphite and Nanotubes. *Phys. Rev. B* **2006**, *73*, 155426-1–155426-6.
24. Farhat, H.; Son, H.; Samsonidze, G. G.; Reich, S.; Dresselhaus, M. S.; Kong, J. Phonon Softening in Individual Metallic Carbon Nanotubes Due to the Kohn Anomaly. *Phys. Rev. Lett.* **2007**, *99*, 145506-1–145506-4.
25. Kalbac, M.; Kavan, L.; Dunsch, L.; Dresselhaus, M. S. Development of the Tangential Mode in the Raman Spectra of SWCNT Bundles During Electrochemical Charging. *Nano Lett.* **2008**, *8*, 1257–1264.
26. Piscanec, S.; Lazzeri, M.; Robertson, J.; Ferrari, A. C.; Mauri, F. Optical Phonons in Carbon Nanotubes: Kohn Anomalies, Peierls Distortions, and Dynamic Effects. *Phys. Rev. B* **2007**, *75*, 035427-1−035427-22.
27. Tarabek, J.; Kavan, L.; Dunsch, L.; Kalbac, M. Chemical States of Electrochemically Doped Single Wall Carbon Nanotubes as Probed by *in Situ* Raman Spectroelectrochemistry and *ex Situ* X-ray Photoelectron Spectroscopy. *J. Phys. Chem. C* **2008**, *112*, 13856–13861.
28. Kukovecz, A.; Pichler, T.; Pfeiffer, R.; Kramberger, C. Kuzmany H Diameter Selective Doping of Single Wall Carbon Nanotubes. *Phys. Chem. Chem. Phys.* **2003**, *5*, 582–587.
29. Kavan, L.; Rapta, P.; Dunsch, L.; Bronikowski, M. J.; Willis, P.; Smalley, R. E. Electrochemical Tuning of Electronic Structure of Single-Walled Carbon Nanotubes: *In-Situ* Raman and Vis-NIR Study. *J. Phys. Chem. B* **2001**, *105*, 10764–10771.